Infrared Spectroscopy of Comet Hale-Bopp

H. A. Weaver
Department of Physics and Astronomy
The Johns Hopkins University
Baltimore, Maryland 21218 USA

T. Y. Brooke
Jet Propulsion Laboratory
Pasadena, CA 91109 USA

G. Chin
NASA Goddard Space Flight Center
Planetary Systems Branch
Greenbelt, MD 20771 USA

S. J. Kim
Kyunghee University
Institute of Natural Sciences
Yongin, Kyunggido 449-701 Korea

D. Bockelée-Morvan
Observatoire de Meudon-Paris
F-92195 Meudon Cedex
France

J. K. Davies
Joint Astronomy Centre
Hilo, Hawaii 96720 USA

(Received ..... ; Accepted in final form .....)

Abstract.
High resolution ($\lambda/\delta\lambda\sim$20,000) spectra of comet C/1995 O1 (Hale-Bopp) in the 2-5 μm region were obtained during UT 2-5 March 1997 using CSHELL at the NASA Infrared Telescope Facility (IRTF) on Mauna Kea. The heliocentric and geocentric distances of the comet were $\sim$1.1 AU and $\sim$1.5 AU, respectively. We detected emission lines of the gas-phase molecules H_2O, CH_4, C_2H_6, C_2H_2, HCN, and CO and derived absolute production rates and relative abundances for all species. We also used the 2-dimensional nature of the CSHELL data to investigate the spatial distribution of the molecules and find evidence that CO was derived at least partly from an extended source in the coma.

Key words: infrared, spectroscopy, composition, comets

1. Introduction

Many cometary parent molecules have strong ro-vibrational transitions in the 1 μm$\leq\lambda\leq$5 μm spectral region. Most of these molecules do not fluoresce strongly at optical and ultraviolet wavelengths, and those lacking permanent electric dipole moments do not radiate strongly at radio wavelengths (including the sub-mm and mm ranges), so spectroscopy in the near-infrared (IR) region can provide unique insights into the composition of cometary nuclei. The advent of sensitive imaging spectrometers in the near-IR now makes it possible to measure abundances in even moderately-bright comets, and the high spatial resolution (typically about $1''$) permits a detailed investigation of the spatial variation in both the column density and the molecular excitation.

On exceptionally bright comets like C/1995 O1 (hereafter referred to as Hale-Bopp), the potential return from near-IR investigations is even greater. In this paper, we report on our observations of Hale-Bopp from the IRTF in Hawaii using the Cryogenic Echelle Spectrometer (CSHELL; Greene et al., 1993). The resolving power of CSHELL varies from $\sim$5,400 to $\sim$43,000 depending on the width of the slit used during the observations. Most of our cometary observations were made using the $1''$ slit, which yields a resolving power of $\sim$20,000 for a source filling the slit in the dispersion direction. All of the CSHELL slits extend $\sim 30''$ perpendicular to dispersion, and analysis of data along this latter direction provides information on the spatial distribution of the emissions. The slit was always oriented with the long dimension (i.e., the spatial dimension) along the celestial east-west direction. During the time of our observations the projected solar vector was at a celestial position angle of $\sim 150°$, and the phase angle (earth-comet-sun) was $\sim 43°$. The spatial resolution of CSHELL depends on the atmospheric conditions but is typically $\sim 1''$. Individual CSHELL pixels are $0\farcs2$ square, which projected to $\sim$200 km at the comet during the time of our observations.

The CSHELL observations were conducted during the mornings and afternoons (local time) of UT 2-5 March 1997. The heliocentric and geocentric distances of the comet were $\sim$1.1 AU and $\sim$1.5 AU, respectively, and the geocentric radial velocity was ~ -24 km s^{-1}. The latter produced a reasonably large doppler shift, which was needed to shift certain cometary emission lines out of the corresponding absorption lines in the terrestrial atmosphere. The observing conditions were excellent during 2-3 March, and we detected gaseous emissions from H_2O, CH_4, C_2H_2, C_2H_6, CO, and HCN. We also detected H_2O, CH_4, and CO on 5 March, despite the presence of intermittent clouds. Only a few useful spectra were obtained on 4 March due to bad weather conditions.

From the observed emission line fluxes, we have calculated molecular production rates and relative abundances. We have also investigated the spatial brightness profiles for each species. Analysis of the spatial profiles is crucial for determining whether the observed species are sublimating from the nucleus, or are primarily produced from an "extended source" in the coma, as was found for CO in comet Halley (Eberhardt et al., 1987).

We performed a sensitive search for other possible parent molecules in comet Hale-Bopp, but that analysis is ongoing and the results will be reported in a future paper.

On 3 March 1997 we obtained complementary near-IR spectra using the Cooled Grating Spectrometer 4 (CGS4) at the United Kingdom Infrared Telescope (UKIRT). A single spectrum covered the entire wavelength range from 3.12 μm to 3.74 μm at a resolving power of $\sim$1500. (Note that an individual CSHELL spectrum only covers a wavelength range of $\sim 2.5 \times 10^{-3} \lambda$, where λ is the central wavelength in the spectrum.) Owing to the strong continuum emission from grains in Hale-Bopp, the CGS4 spectra show no clear evidence of any molecular emissions. For the purpose of the current paper, the CGS4 spectra are mainly used to provide a broad overview of Hale-Bopp's IR spectrum and to check CSHELL's absolute calibration. A more detailed discussion of the UKIRT program on Hale-Bopp will be given elsewhere (Davies et al., in preparation).

2. Spectra

Due to CSHELL's limited free spectral range, the observations of Hale-Bopp were obtained at many different grating settings. Observations of calibration stars, flat-fields, and darks were also obtained at each grating setting. For the stellar observations, we generally used the $4''$ slit in order to ensure that all of the stellar flux was collected. The known absolute flux of the star and its observed count rate allowed us to transform the observed cometary count rates into absolute units (but, at this point, still not corrected for terrestrial absorption).

Prior to any spectroscopic observation, a mirror was moved in front of the grating so that we could verify by direct imaging that the object (either the comet or the star) was centered in the slit. Typically, we would integrate on the target for 1 minute, offset 3 arcmin and integrate 1 minute for a background measurement, and then re-check the pointing. It was common for the target to move by $\sim 0\farcs5$ during the course of our observations. Such motions caused variations of $\sim$20-30% in the observed cometary signal, and this is thought to be the dominant source of error in our derived fluxes and production rates. Using a wider slit would have reduced our susceptibility to pointing uncertainties, but a narrow slit was needed for the cometary observations to improve the line-to-continuum contrast.

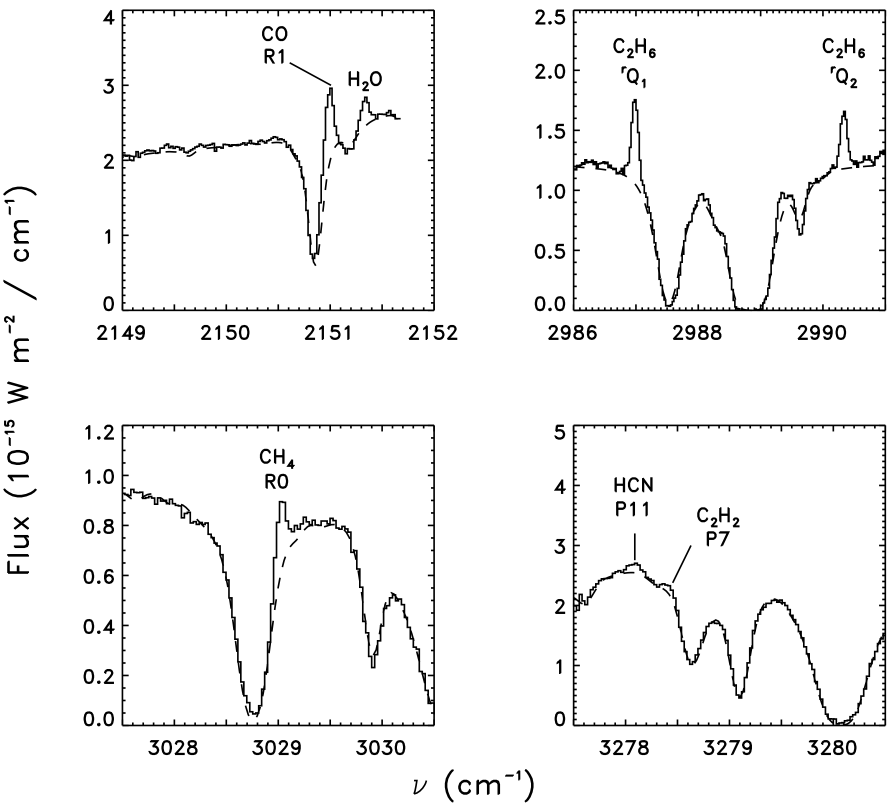

Figure 1. The plots show flux-calibrated spectra in the regions having gaseous emissions from CO, H_2O (the $1_{11} - 1_{10}$ line in the $\nu_3 - \nu_2$ band), C_2H_6, CH_4, HCN, and C_2H_2. The spectra have not been corrected for atmospheric transmittance; gases in the terrestrial atmosphere produce the many observed absorption features. The effective aperture size is $1'' \times 2''$ ($1'' \times 5''$ for the HCN-C_2H_2 region), and it was approximately centered on the nucleus. The gaseous emissions are superimposed on a strong continuum emitted by the cometary grains, which we have modeled (dashed lines). The CO-H_2O spectrum was taken on 5 Mar 1997 through clouds, so the absolute fluxes are not accurate in this case. All other spectra were taken on 2 Mar 1997 under good weather conditions.

Examples of portions of our calibrated CSHELL spectra are shown in figures 1 and 2. Emissions from CO, H_2O, C_2H_6, and CH_4 were easily detected during 1 min (on-source) exposures. The HCN-C_2H_2 spectrum is an average of four exposures with a total on-source integration time of 7 min.

The terrestrial atmospheric transmittance was calculated for the observational conditions using FASCOD2 (Clough et al., 1986). The transmittance was then multiplied by a function that varied slowly and smoothly with wavenumber so that a good match was obtained with the observed flux-calibrated cometary spectrum. This scaled transmittance spectrum is the estimated cometary continuum. Subtraction of this model continuum from the observed spectrum yielded the "emission line" spectra plotted in figure 2. Integration of the emission line over wavenumber gives the observed line-integrated flux, which is then divided by the calculated atmospheric transmittance at the doppler-shifted position of the cometary line to yield the flux at the top of the atmosphere.

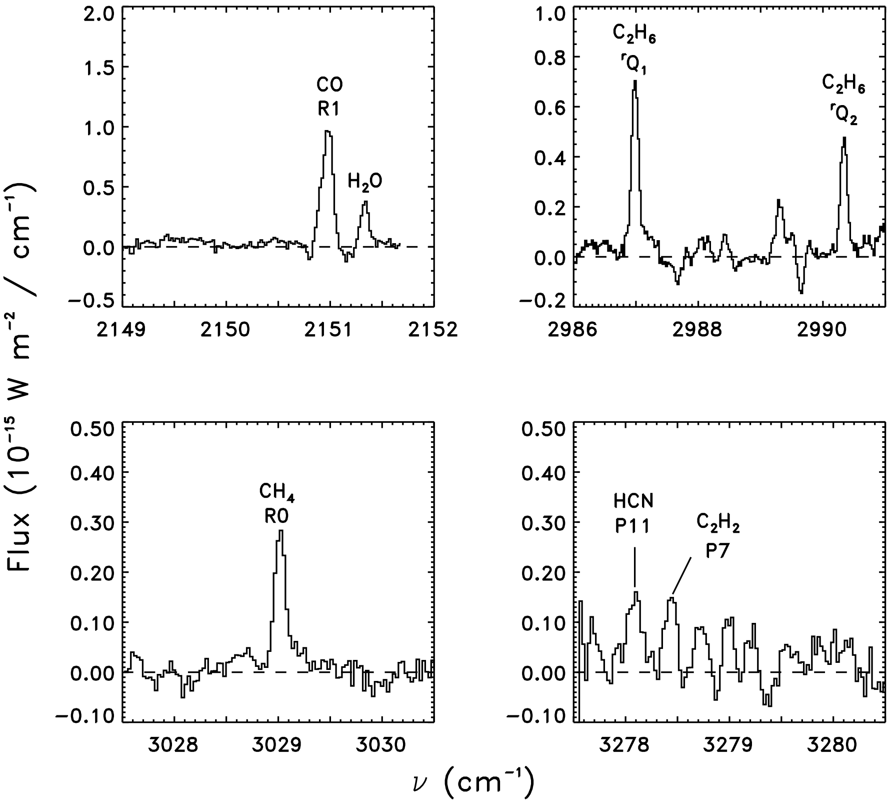

Figure 2. These are emission-line spectra produced by subtracting the model continua in figure 1 from their corresponding cometary spectra. Note that the detections of HCN and C_2H_2 are more secure than they appear; the noise in the regions of strong terrestrial atmospheric absorption is larger than that in the regions of high transmittance, where the HCN and C_2H_2 lines lie.

3. Spatial Profiles

One major advantage of CSHELL for cometary observations is the ability to obtain spatially-resolved spectra with a resolution of $\sim 1''$. The spatial profile for the continuum was obtained by averaging five columns in a region that contained only continuum emission. (The columns in the spectral image run perpendicular to the dispersion direction and the rows run parallel to dispersion.) Spatial profiles for the gaseous emissions were extracted using two different techniques. In the first, five columns centered on the emission feature were averaged and a scaled continuum spatial profile was subtracted from it. In the second method, the model cometary continuum spectrum was subtracted row-by-row from the observed spectral image producing an "emission" spectral image. Then five columns in this latter image were averaged to produce the spatial profile for the molecular emission. The two techniques give essentially identical results at distances greater than $\sim$15 pixels ($3''$) from the nucleus. In the inner coma, the results from the first method depend sensitively on the relative alignment of the two steeply-sloped spatial profiles and on the precise value used to scale the continuum profile. Thus, we favor the second approach and present those results here (fig. 3).

As expected, all the cometary emissions have a broader spatial profile than that of the star. Except for H_2O and CO, the spatial profiles are fairly symmetrical about their peak emission. The H_2O profile is slightly higher in the westward-facing coma while the CO profile is higher in the eastward-facing coma. On the eastward side, the H_2O profile follows the continuum profile fairly closely, while there appears to be an extra "bulge" of H_2O on the westward side. CO is the only cometary gaseous emission whose spatial profile clearly deviates from that of the continuum over most of the coma, indicating that much of the observed CO does not sublimate directly from the nucleus. We have plotted the spatial profile for a single CO line, and it is possible that the observed spatial brightness distribution reflects a change in the molecular excitation as a function of cometocentric distance rather than a change in the column density (cf., Chin & Weaver, 1984). However, no such excitation effects are clearly evident in the spatial profiles of the other molecular emissions, and the spatial profile for the CO R1 line (not shown) is also much flatter than the continuum profile. We also detected the CO R3, R5, and R6 lines but have not yet analyzed their spatial distributions.

As discussed in the next section, the CO line at small cometocentric distances is optically thick. However, the CO profile shows little sign of steepening even in the outer coma where optical depth effects should be significantly reduced. We also note that the H_2O line suffers from opacity effects, yet still has a profile that is more similar to that of the continuum (i.e., the canonical profile for parent molecules) than to that of CO. We conclude that, like the case for comet Halley, the CO

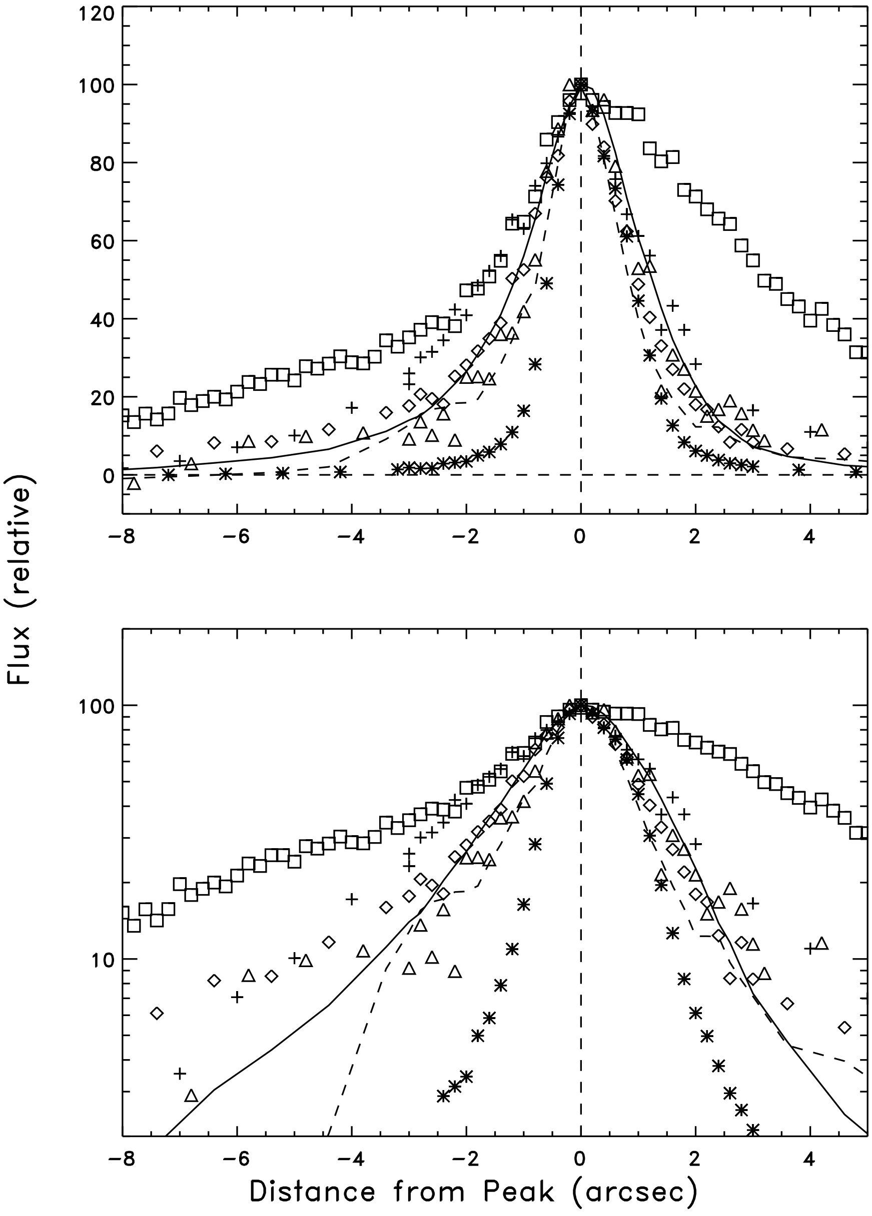

Figure 3. Spatial brightness profiles are plotted for CO (□), H_2O (+), C_2H_6 (◇), CH_4 (△), the cometary continuum in the CO region (solid line), the cometary continuum in the C_2H_6 region (dashed line), and for a star (*). The top panel shows the data on a linear plot, while the data are displayed on a semi-log plot in the bottom panel. In both cases, celestial west points to the left and east points to the right.

in the coma of Hale-Bopp is derived at least partly from a non-nuclear source. Thus, caution is advised when comparing CO production rates derived from different observations that subtend different cometocentric distances.

4. Abundances

From the observed absolute fluxes in a $1'' \times 2''$ aperture, we have derived molecular production rates (Qs) for H_2O, CH_4, C_2H_2, C_2H_6, CO, and HCN (Table 1). We assumed that all species are parent molecules flowing outward from the nucleus with a speed of 0.8 km s^{-1} and have ignored lifetime effects, which should be negligible for our observations. We converted observed fluxes to column densities assuming optically thin conditions (but see the further discussion on CO below), except for the case of H_2O for which we used a detailed molecular excitation model that includes radiative transfer using the escape-to-space formalism (Bockelée-Morvan, 1987). The g-factors (at $r = 1$ AU, Table 1) are LTE values for a temperature of 100 K, which is consistent with the estimated kinetic temperature derived by Biver et al. (1998). The CH_4 and CO g-factors are especially sensitive to the assumed temperature; eventually we will use our measurements of the relative intensities of multiple lines in the same band to derive our own estimate of the temperature.

As discussed earlier, at least some of the CO probably comes from an extended source, which means that the quoted CO production rate is only an upper limit to the true value at the nucleus. However, the listed production rate implies an aperture-averaged column density of $\sim 4 \times 10^{16}$ mol cm^{-2}, which means that the observed CO lines are optically thick for lines of sight passing near the nucleus (with τ of order 10). The effect of opacity is to cause us to underestimate Q_{CO}. In principle, we could use the column brightness at large distances from the nucleus, where the emission should become optically thin, to derive an accurate value for Q_{CO}. At a distance of $5''$ from the nucleus, the column density of a parent molecule should be a factor of $\sim$13 times smaller than the aperture-averaged value at the nucleus. If we use the observed CO brightness at an offset of $5''$ and assume that all the CO is being produced via sublimation at the nucleus, then Q_{CO} would be increased by a factor of $\sim$3 compared to the value listed in the table and would then be comparable to the Q_{CO} values derived from sub-mm (Biver et al., 1998) and ultraviolet (Feldman, 1998) observations. However, the CO brightness profile is still relatively flat for offset distances between $5''$ and $8''$, indicating that the value of Q_{CO} derived in this way is overestimated because at least some (and maybe most) of the CO is being produced from an extended source in the coma, as discussed in the previous section. Until these issues are addressed more carefully, the value of Q_{CO} listed in Table 1 should be treated as a preliminary estimate.

The C_2H_6 and CH_4 abundances listed in Table 1 are similar to the values derived for comet Hyakutake (C/1996 B2; Mumma et al., 1996; Weaver et al., 1999). The HCN abundance is consistent with that derived at a similar heliocentric distance from radio observations of Hale-Bopp (Biver et al., 1998) and with the range of values observed in other comets (cf., Bockelée-Morvan, 1997). The C_2H_2 abundance listed in Table 1 is somewhat lower than the value derived for Hyakutake ($0.3 - 0.9$; Brooke et al., 1996).

Table I. Molecular Abundances†

Line ID	ν	g-factor	Flux	Q	Abundance
C_2H_6 $^rQ_1$	2986.749	3.4	12	0.24	0.48
CH_4 R0	3028.752	1.7	8.2	0.31	0.62
CO R2	2154.596	1.4	84	5.2	10
H_2O $1_{11} - 1_{10}$	2151.194	0.045	23	50‡	100
HCN P8	3287.248	2.0	2.8	0.085	0.17
C_2H_2 P7	3278.190	1.6	1.2	0.046	0.09

†The rest frequencies (ν) of the observed lines are given in cm^{-1}, the g-factors have units of 10^{-5} photons s^{-1} molecule^{-1}, the flux has units of 10^{-17} W m^{-2}, the production rates (Q) have units of 10^{29} molecules s^{-1}, and the abundances are in percent relative to H_2O. The listed H_2O line is in the $\nu_3 - \nu_2$ band. The data listed generally refer to a single observation. We have multiple observations (sometimes on different days) for several species, but those data have not yet been fully reduced.

‡For a measurement of a H_2O line obtained on 1.9 March 1997 from the IRTF, Dello Russo et al. (1998) give 54 ± 3. Based on OH radio observations, Colom et al. (1998) give 37 (+1.8,−0.4) as an average value for the period 1-7 March 1997. The value in the table is derived from our IRTF observations of the listed H_2O line.

Acknowledgements

We thank Don Yeomans for providing timely ephemeris support, Tom Geballe for participating in the UKIRT observations, and the IRTF and UKIRT telescope operators for their expert assistance in executing the observations. H. A. Weaver gratefully acknowledges financial support for his work from NSF grant number 9615605 to the Johns Hopkins University. S. J. Kim acknowledges financial support through grants from the Korean Science and Engineering Foundation (KOSEF 96-0702-03-02-3) and the Korean Research Foundation.

References

Biver, N., et al.: 1998,'Long-term evolution of the outgassing of comet Hale-Bopp from radio observations', *Earth, Moon, Planets*, TBD, TBD-TBD

Bockelèe-Morvan, D.: 1987, 'A model for the excitation of water in comets', *Astron. Astrophys.*, **181**, 169-181

Bockelèe-Morvan, D.: 1987, 'Cometary Volatiles : The status after comet C/1996 B2 Hyakutake', in *Molecules in Astrophysics: Probes and Processes*, E. F. van Dishoeck (ed.), IAU Symposium No. 178, Kluwer, 219-235

Bockelèe-Morvan, D. & Crovisier, J.: 1988, 'The nature of the 2.8 μm feature in cometary spectra', *Astron. Astrophys.*, **216**, 278-283

Brooke, T. Y., et al.: 1996, 'Detection of acetylene in the infrared spectrum of comet Hyakutake', *Nature*, **383**, 606-608

Chin, G. & Weaver, H. A.: 1984, 'Vibrational and rotational excitation of CO in comets: nonequilibrium calculations', *Ap. J.*, **285**, 858-869

Clough, S. A., Kneizys, F. X., Shettle, E. P., & Anderson, G. P.: 1986, 'Atmospheric radiance and transmittance: FASCOD2', in *Proc. Sixth Conf. Atmos. Radiation*, American Met. Soc., 141-144

Colom, P., et al.: 1998, 'Observations of the OH radical in comet Hale-Bopp with the Nançay radio telescope', *Earth, Moon, Planets*, TBD, TBD-TBD

Dello Russo, N., et al.: 1998, 'Quantification of water and carbonyl sulfide in comet Hale-Bopp using ground-based infrared spectroscopy', *Earth, Moon, Planets*, TBD, TBD-TBD

Feldman, P. D.: 1998, 'Ultraviolet observations of comet Hale-Bopp', *Earth, Moon, Planets*, TBD, TBD-TBD

Eberhardt, P., et al.: 1987, 'The CO and N_2 abundance in comet P/Halley', *Astron. Astrophys.*, **187**, 481-484

Greene, T. P., Tokunaga, A. T., Toomey, D. W., & Carr, J. S.: 1993, 'CSHELL: A high spectral resolution 1–5 micron cryogenic echelle spectrograph for the IRTF', *Proc. SPIE*, **1946**, 313-324

Mumma, M. J., et al.: 1996, 'Detection of Abundance Ethane and Methane, Along with Carbon Monoxide and Water, in Comet C/1996 B2 Hyakutake: Evidence for Interstellar Origin', *Science*, **272**, 1310-1314

Weaver, H. A., et al.: 1999, 'The Methane Abundance in Comet Hyakutake (C/1996 B2)', *Ap. J.*, to be submitted

Address for correspondence: Department of Physics and Astronomy, The Johns Hopkins University, Baltimore, Maryland 21218 USA, weaver@pha.jhu.edu